



Contents lists available at ScienceDirect

Fundamental Research

journal homepage: <http://www.keaipublishing.com/en/journals/fundamental-research/>

Review

The application of aromaticity and antiaromaticity to reaction mechanisms

Qin Zhu^{a,b}, Shuwen Chen^a, Dandan Chen^a, Lu Lin^a, Kui Xiao^c, Liang Zhao^c, Miquel Solà^d, Jun Zhu^{a,e,*}^a State Key Laboratory of Physical Chemistry of Solid Surfaces and Collaborative Innovation Center of Chemistry for Energy Materials (iChEM), College of Chemistry and Chemical Engineering, Xiamen University, Xiamen 361005, China^b Key Laboratory for Organic Electronics & Information Displays (KLOEID) and Institute of Advanced Materials (IAM), SICAM, Nanjing University of Posts & Telecommunications, Nanjing 210023, China^c Key Laboratory of Bioorganic Phosphorus Chemistry and Chemical Biology (Ministry of Education), Department of Chemistry, Tsinghua University, Beijing 100084, China^d Institute of Computational Chemistry and Catalysis and Department of Chemistry, University of Girona, C/ M. Aurèlia Capmany, 69, 17003 Girona, Catalonia, Spain^e School of Science and Engineering, The Chinese University of Hong Kong, Shenzhen 518172, China

ARTICLE INFO

Article history:

Received 14 January 2023

Received in revised form 31 March 2023

Accepted 24 April 2023

Available online 28 April 2023

Keywords:

Aromaticity

Antiaromaticity

Reaction mechanism

Frustrated Lewis pairs

Dinitrogen activation

Small molecule activation

ABSTRACT

Aromaticity, in general, can promote a given reaction by stabilizing a transition state or a product via a mobility of π electrons in a cyclic structure. Similarly, such a promotion could be also achieved by destabilizing an antiaromatic reactant. However, both aromaticity and transition states cannot be directly measured in experiment. Thus, computational chemistry has been becoming a key tool to understand the aromaticity-driven reaction mechanisms. In this review, we will analyze the relationship between aromaticity and reaction mechanism to highlight the importance of density functional theory calculations and present it according to an approach via either aromatizing a transition state/product or destabilizing a reactant by antiaromaticity. Specifically, we will start with a particularly challenging example of dinitrogen activation followed by other small-molecule activation, C–F bond activation, rearrangement, as well as metathesis reactions. In addition, antiaromaticity-promoted dihydrogen activation, CO₂ capture, and oxygen reduction reactions will be also briefly discussed. Finally, caution must be cast as the magnitude of the aromaticity in the transition states is not particularly high in most cases. Thus, a proof of an adequate electron delocalization rather than a complete ring current is recommended to support the relatively weak aromaticity in these transition states.

1. Introduction

Aromatics exhibit numerous applications to various fields, including biomedicine, materials science, energy science and environmental science [1]. Aromaticity, as the footstone of aromatic chemistry as well as one of the most important concepts in chemistry, can be used to rationalize reaction mechanisms due to electron delocalization caused by bond length equalization in an intermediate, transition state or a product [2,3]. For example, a summary of the application of this concept to organic reactions was reported by Zimmerman as early as 1971 [4]. Very recently, the role of aromaticity in Diels–Alder reactions was summarized by Houk and co-workers [5]. However, the important role of aromaticity in the transition state has been overlooked to some extent. As both aromaticity and transition state cannot be directly measured experimentally, computational chemistry has been an effective tool to quantify and understand the aromaticity in a transition state. Early in 1939, Evans pointed out “the greater the mobility of the π electrons in the

transition state, the greater will be the lowering of the activation energy” [6]. However, to the best of our knowledge, only one review involving aromaticity in the transition state was published in 2014 by Cossío, Fernández, and co-workers [7], focusing on pericyclic and pseudo-pericyclic reactions. Therefore, in this review, we mainly focus on the recent development of aromaticity-driven reactions in the past nine years (2015–2023) with the emphasis on the stabilization of transition states.

Hückel’s rule states that monocyclic π -conjugated systems with $4n + 2$ π -electrons are aromatic in the ground state, which has been fully developed in organic chemistry. In contrast, Baird’s rule states that species with $4n + 2$ π -electrons are antiaromatic in the lowest triplet state and those with $4n$ π -electrons are aromatic [8]. Excited-state aromaticity could become a cornerstone for photochemistry but is less developed [9,10]. Currently, excited-state (anti)aromaticity can be used to explain some observations of photophysical and photochemical behaviors [11–13]. For instance, excited-state antiaromaticity has an important effect on the photoinduced proton-coupled-electron-transfer

* Corresponding author.

E-mail address: jun.zhu@xmu.edu.cn (J. Zhu).<https://doi.org/10.1016/j.fmre.2023.04.004>2667-3258/© 2023 The Authors. Publishing Services by Elsevier B.V. on behalf of KeAi Communications Co. Ltd. This is an open access article under the CC BY-NC-ND license (<http://creativecommons.org/licenses/by-nc-nd/4.0/>)

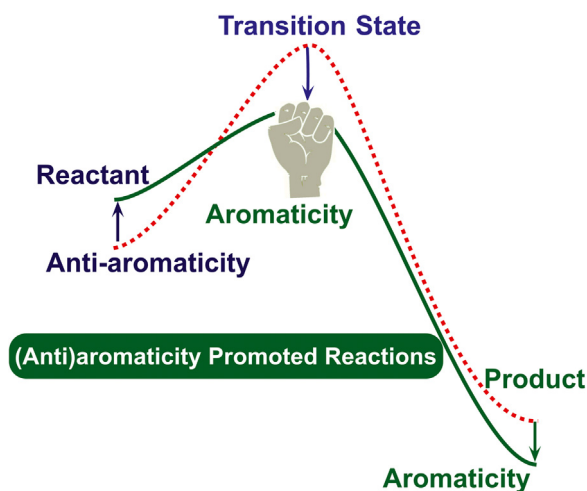


Fig. 1. Illustration of strategies for (anti)aromaticity-driven reaction via enabling an antiaromatic reactant or aromatizing a transition state/product.

(PCET) [14] and the electrocyclization of dithienylbenzene switches [15]. Singlet fission is a photophysical process where an organic chromophore absorbs one photon and splits a high-energy singlet exciton into two relatively low-energy triplet excitons, and excited-state aromaticity plays an important role in the search of novel singlet fission materials [16]. The experimental assessment of excited-state aromaticity in the expanded porphyrins was realized and further verified by time-resolved optical spectroscopic measurements [17].

On the other hand, aromaticity also exhibits important applications in reaction mechanisms, such as in the mechanisms of small-molecule activation, cycloaddition reactions, intramolecular rearrangements, isomerization, electrocyclic reactions, [1, X]-shift reactions as well as aromaticity-driven metallacycle syntheses. Taking small-molecule activation as an example, the main components in the atmosphere (N_2 and O_2) can be used to construct value-added species containing C–N or C–O bonds and the methane in natural gas can be activated to form valuable chemicals [18]. Moreover, the capture and sequestration of environmentally unfriendly small molecules such as CO_2 and CS_2 are important projects to achieve green chemistry. Great progress in small-molecule activation has been made by transition metal complexes due to the appropriate energy and symmetry of the d orbitals of transition metals [19]. Over the last decades, main-group species have also shown great potential in small-molecule activation, such as frustrated Lewis pairs (FLPs) [20], main-group pincer compounds [21], low-valent species of groups 13 and 14 elements [22] and singlet carbenes [23]. However, most of these reactions in small-molecule activation involve cyclic transition states or products and their aromaticity has not received adequate attention.

In this review, we will analyze the relationship between the reaction mechanism and aromaticity and discuss it according to an approach via either stabilizing a transition state/product by aromaticity or destabilizing a reactant by antiaromaticity, as illustrated in Fig. 1. Specifically, enabling an antiaromatic reactant will facilitate a reaction both kinetically and thermodynamically in most cases, whereas aromaticity gained or enhanced in a transition state promotes a reaction kinetically and that in a product does thermodynamically.

2. A procedure for the selection of an aromaticity index

Many aromaticity descriptors have been proposed on the basis of multiple manifestations of aromaticity [24]. However, one must utilize a set instead of a single one to justify aromaticity in a given system [25–27]. Choosing the “right” aromaticity descriptors is not a trivial task,

whereas under many circumstances, we should perform all the suitable methods to determine if some aromaticity indices reach the same conclusion or correlate well with each other. Note that aromaticity indices are not always consistent with each other. In most cases, the contradictions are mainly caused by the incorrect use of some indices rather than the multidimensional nature of aromaticity. In our opinion, as the nature of aromaticity is electron delocalization, electronic indices should have a top priority. Then other aromaticity indices based on geometric, energetic, and magnetic properties could be considered in sequence. A general procedure including a few steps is personally suggested to evaluate aromaticity in a simple but efficient manner (Fig. 2). Long-range corrected density functionals (e.g., CAM-B3LYP and ω B97XD) have better performance in the evaluation of electron delocalization [28]. For geometry optimization of transition metal-containing complexes, we usually use B3LYP, TPSS, PBE0, M06L, etc., together with the ECP n MDF basis sets (n is the number of core electrons) with fully relativistic effective core potentials (ECPs) for heavy transition metal systems.

The electron density of delocalized bonds (EDDB) method [29] can be used for almost all types of systems. EDDB measures electron delocalization quantitatively, with the capability of dissection into components based on orbital symmetries (σ , π , δ , etc.), open-shell α/β subspaces, molecular fragments, designated paths, and atomic and orbital contributions. To distinguish between nonaromaticity and antiaromaticity, the electron localization function (ELF) is recommended [30], especially for planar systems. As long as we obtain the optimized structure of a system, it is always recommended to check the difference between the longest and the shortest bonds (Δ BL). Δ BL is the most direct index for bond equalization, but the investigated bonds must be of the same nature. Although EDDB and Δ BL are listed only for a few cases in Fig. 2, these two methods can be used for almost every type of cyclic structures.

For small rings, the multicenter index (MCI) [30] is one of the most popular aromaticity descriptors based on electron delocalization. The normalized form, $MCI^{1/n}$ (n is the number of ring atoms), can be used to compare aromaticity between rings with various sizes. Since each MCI analysis involves $(n-1)!$ calculations, it is not recommended for large rings ($n > 12$). Magnetic indices, such as nucleus-independent chemical shift (NICS) [31], isochemical-shielding surface (ICSS) [32], anisotropy of the current-induced density (ACID) [33], and gauge-including magnetically induced current (GIMIC) [34] are suitable for planar systems, as it is much easier to align an external magnetic field perpendicular to the molecular plane. NICS is one of the most widely used aromaticity descriptor. However, it should be carefully analyzed in transition metal systems, as the extreme deshielding of the light atoms in the vicinity of the osmium atoms in osmapentalene derivatives could be caused by paramagnetic couplings between σ_{Os-C} bonding orbitals and the π^*_{Os} orbitals rather than aromaticity [35]. The ICSS can characterize aromatic and antiaromatic rings by shielding and deshielding cones, respectively. Both the ACID and GIMIC provide visualization of diatropic ring currents in aromatic systems and paratropic ring currents in antiaromatics.

Finally, the harmonic oscillator measure of aromaticity (HOMA) [36] could be used for non-metal systems and the isomerization stabilization energy (ISE) [37] for all-carbon, heterocyclic, and organometallic systems. It is impossible to use HOMA for all-metal systems, as it requires the parameterization of metal-containing bonds, which is not available to date. ISE depends on the definition of a reference system, for which no designs for all-metal systems have been proposed in the literature.

3. Aromaticity-stabilized transition states in triple bond activation

As we mentioned before, the approach for aromaticity-driven reactions could be divided into aromatizing a transition state/product or destabilizing a reactant by antiaromaticity. We start with a discussion of aromaticity-stabilized transition states. In this section, some key achievements in aromaticity-driven triple bond activation are summa-

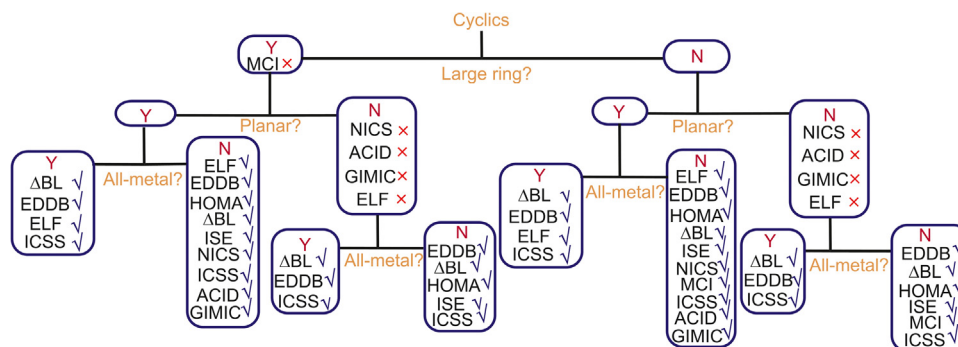


Fig. 2. A proposed procedure for selection of an aromaticity index. Y: Yes; N: No. ✓ means the aromaticity index is suggested for this system whereas “×” is not. EDDB, ICSS and Δ BL can be used for almost all systems. ELF can distinguish nonaromaticity and antiaromaticity in planar systems. MCI is recommended for small rings whereas NICS, ACID, and GIMIC are suitable for planar systems. HOMA can be used for non-metal system and ISE for all-carbon, heterocyclic, and organometallic systems.

alized first. The functionalization of dinitrogen (N_2) under mild conditions is one of the most significant challenges in chemistry due to the remarkably strong and non-polar $N\equiv N$ triple bond. Dinitrogen activation has been achieved by either boron species or metallic systems via mononuclear or polynuclear metal complexes [38]. However, the development of main-group elements for N_2 fixation or activation remains limited [39,40]. Recently, some of us proposed a new strategy that combines the concept of aromaticity with FLPs for N_2 activation for the first time [41]. It is found that the combination of a methyleneborane with a N-heterocyclic carbene could achieve metal-free N_2 activation (Fig. 3a). Mechanistic studies reveal that such metal-free N_2 activation is favorable both kinetically and thermodynamically (with an activation energy as low as $9.1 \text{ kcal mol}^{-1}$ and an exothermicity of $18.9 \text{ kcal mol}^{-1}$). In general, a distinctly negative NICS value suggests aromaticity, and a distinctly positive one means antiaromaticity. The calculated $NICS(1)_{zz}$ values and ACID results show that the number of aromatic rings in this process gradually increased from one in the reactant to two in the transition state and to three in the product, highlighting a crucial role of aromaticity in N_2 activation in this system. Interestingly, when two rings in the product (5) become nonaromatic, the reaction becomes endergonic (Fig. 3a) [41].

The cleavage of $C\equiv N$ triple bond has attracted great interest for its wide application in organic synthesis. Xi, Takahashi, and co-workers discovered that in the presence of two molecules of MeCN, one of the Cp units on titanacyclopentadiene $Cp_2Ti(C_4Et_4)$ (6) was cleaved into a two-carbon unit and a three-carbon unit (Fig. 3b), which were converted into a benzene derivative (11) and a pyridine derivative (12), respectively [42]. This reaction involves the cleavage of two $C=C$ double bonds and one $C\equiv N$ triple bond. Suresh and Koga investigated the reaction mechanism by density functional theory (DFT) calculations [43]. Results show that the titanium nitride intermediate was stabilized by the formation of an aromatic titanacycle. The formation of 6π -electron metallaheterocycles 8 and 10 was an aromaticity-driven step with low reaction barriers. Delocalized electronic structures, energetic stabilization, and negative $NICS(0)$ values in 7-TS (-4.8 ppm), 8 (-9.2 ppm), 9-TS (-7.1 ppm), and 10 (-9.0 ppm), indicate that aromaticity plays an important role in the stabilization of the intermediate and transition states in this unique process.

Alkyne, containing a $C\equiv C$ triple bond, is also an important synthon in synthetic chemistry. The aromatic system with a $C\equiv C$ triple bond, aryne, is an active intermediate. Hoye et al. reported post-aromatization of a hexadehydro-Diels-Alder reaction (HDDA) of triynes or tetraynes (Fig. 3c) [44]. DFT calculations show that cycloaromatization of the triyne approach to the ortho-benzyne intermediate (16) was exothermic by $-51.4 \text{ kcal mol}^{-1}$, and the trapping step to form 17 by *t*-butanol of the strained alkyne was exothermic by $-73.0 \text{ kcal mol}^{-1}$. The formation of a benzyne intermediate from triyne or tetrayne substrates in

this reaction could be viewed as an aromaticity-driven process. Subsequently, they found that the aromaticity-driven HDDA reaction can be extended to alkane desaturated reaction [45]. As shown in Fig. 3c, the HDDA-generated benzyne intermediate (19) accepts two hydrogen atoms from a saturated alkane, leading to the formation of the corresponding benzenoid product (20) and alkene. This study shows that the benzyne intermediate is capable of concerted deprotonation of a hydrocarbon. Interestingly, DFT calculations indicate that these reactions have relatively low reaction activation barriers via in-plane aromatic transition states (22-TS) (Fig. 3d). The negative NICS values ranging from -10.0 to -20.8 ppm computed at the (3,+1) ring critical point and diatropic ring current in an ACID plot confirmed the aromaticity of transition states [46].

4. Aromaticity-stabilized transition states in double bond activation

Transition metal-catalyzed olefin metathesis is an important reaction in organic synthesis and material science. However, the metathesis between $C=O$ and $C=C$ double bonds has been less developed. Some of us performed a DFT study on an iron(III)-catalyzed carbonyl-olefin metathesis (COM) reaction by introducing the concept of hyperconjugative aromaticity in the transition state and product (Fig. 3e) [47]. The concerted cycloreversion step from 27 to 28 was found to be strongly related to aromaticity. Lowering activation energy of the cycloreversion step is closely related to the aromatic character of the transition state (27-TS) caused by hyperconjugation, which was supported by the larger π -EDDB (0.987 e) of the five-membered ring (5MR) and MCI values (0.462). This study shows that the hyperconjugative aromaticity of transition states could play an important role in this COM reaction.

Recently, some of us reported an aromaticity-promoted CO_2 activation by a heterocyclopentadiene-bridged P/N-FLPs system [48]. In the open form of P/N-FLPs, the increase of aromaticity determines the activation energy in the reaction. The activation energies for aromatic furan- or pyrrole-bridged FLPs 29 and 31 were in the range of 5.4 – $7.7 \text{ kcal mol}^{-1}$. The aromaticity of transition states and the products was evaluated by NICS and ACID analyses (Fig. 3f). The calculated $NICS(1)_{zz}$ values for the 5MR were gradually increased in the reactant (-9.1 and -9.4 ppm for 29 and 31, respectively) to the transition state (-14.1 and -14.6 ppm for 29-TS and 31-TS, respectively) and to the product (-23.3 and -26.6 ppm for 30 and 32, respectively), indicating that the aromaticity plays an important role in the reaction. Interestingly, the investigation of CS_2 activation through a heterocyclopentadiene-bridged P/N-FLPs system drew the same conclusion. It's worth noting that the CO_2 activation is more efficient than that of CS_2 through a comparative DFT study with CO_2 capture [49]. It could be attributed to the elec-

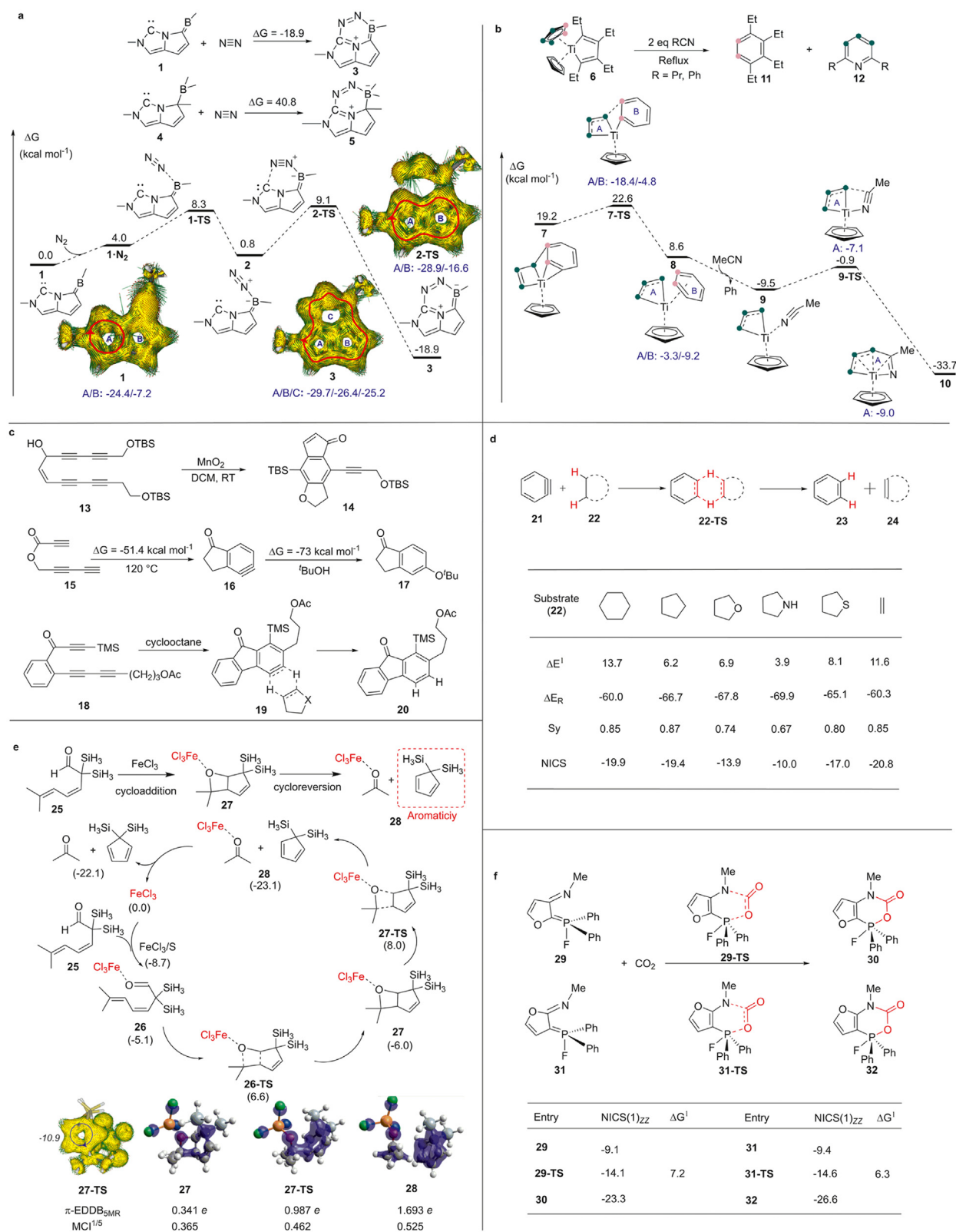


Fig. 3. Aromaticity-stabilized transition states in triple or double bond activation. (a) Gibbs energy profiles of the N₂ fixation by carbon-boron FLPs together with the NICS(1)_{zz} values (in ppm) in blue [41]. Computational method, ωB97XD/cc-pVTZ. (b) Activation of the C≡N triple bond in MeCN. Ethyl and R group were replaced for H and methyl in DFT calculation [42,43]. NICS(0) values given (in ppm) in blue. Computational method, B3LYP/6–31(G)(LanL2DZ). (c) HDDA of triyne or tetrayne [44,45]. Computational method, M06–2X/6–31+G(d,p). (d) Electron barrier and reaction energies for the reaction of benzyne with cyclic hydrocarbon (ΔE[‡] and ΔE_R, in kcal mol⁻¹, Synchronicities (Sy), and NICS (in ppm) computed at the [3,+1] ring critical point [46]. Computational method, M06–2X/6–31+G(d,p). (e) Gibbs energy profile and aromaticity analyses (ACID plots, EDDB isosurfaces and MCI analysis) in the cycloreversion step [47]. Computational method, SMD(dichloroethane)-(U)ωB97XD/def2-TZVP//((U)B3LYP-D3(BJ)/6–31G(d) (LanL2DZ). Isovalues for EDDB and ACID are 0.01 and 0.035, respectively. The NICS(1)_{zz} values of the five membered-rings (5MRs) in ppm. (f) NICS(1)_{zz} values (ppm) in the 5MR and Gibbs energy barrier (kcal mol⁻¹) for CO₂ capture by hetero-cyclopentadiene [48]. Computational method, M06–2X/6–31+G(d).

trostatic attraction between FLP and CO₂ rather than the electrostatic repulsion caused by the reversed polarity of C=S in CS₂.

5. Aromaticity-stabilized transition states in single bond activation

Recent studies have revealed that the aromaticity of the transition-state also plays a dominating role in the single bond activation and isomerization. For instance, a metal-free C–H allylation was achieved by the iodane-guided “iodonio-Claisen” allyl transfer of hypervalent (diacetoxy)iodoarenes [50]. In the mechanism of this reaction, an aromatic transition state for the [3,3] sigmatropic rearrangement was proposed and confirmed by DFT calculations (Fig. 4a). The synchronicity (Sy) value (0.83), diatropic induced ring currents in ACID analysis, negative NICS(0)_{zz} and NICS(1)_{zz} values (−16.3 and −14.3 ppm) support the aromaticity of the iodine-containing six-membered ring (6MR) transition state.

In comparison with numerous approaches to C–H bond activation, the C–F bond activation has also attracted considerable attention from scientists [51]. However, the activation of C–F is challenging, which might be attributed to the high bond dissociation energy (e.g., 109 kcal mol^{−1} for CH₃–F). Although different strategies have been developed for the C–F bond activation, the aromaticity-driven C–F bond activation is less developed. Recently, some of us found aromaticity-promoted C–F bond activation in the tautomerization of a rhodium complex (Fig. 4b) [52]. The aromaticity in the transition states and the products was indicated by the calculated negative NICS(0) values (−22.0 and −25.0 ppm) and small bond length alternations (ΔBLs, 0.027 and 0.036 Å) values of the Cp* ring in **40-TS** and **41**, which makes the tautomerization both thermodynamically favorable and kinetically feasible. This study highlights an important role of aromaticity in C–F bond activation via the stabilization of transition states and products.

In addition, some of us found that the aromaticity also played an important role in the [1,5]-migration of pyrrolium derivatives (Fig. 4c) [53]. Although the N–Au (98.8 kcal mol^{−1}) and N–Sn (81.7 kcal mol^{−1}) bonds have higher bond dissociation energies than the N–F bond (57.6 kcal mol^{−1}), they have lower activation barriers (4.5 and 4.9 kcal mol^{−1} for AuPMe₃ and SnH₃, respectively) than the N–F bond in the [1,5]-migration of pyrrolium derivatives. This unexpected phenomenon could be attributed to the aromatic stabilization of the transition states. The [1,5]-migration of pyrrolium derivatives shows that the synergistic effect of aromaticity, bond strength, and frontier molecular orbital determines the activation energies and reaction energies. It should be noted that aromatic-promoted [1,5]-migrations were also observed previously [54,55]. For instance, Alabugin and co-workers found that the NICS(1) value for the transition state in [1,5]-migration was negative, which was consistent with the facile thermodynamics and kinetics process [54]. Electropositive migratory groups were found to reduce the [1,5]-migration activation energies due to the aromatic character of the transition states [55]. In addition, some of us also found that aromaticity can be used to explain the thermodynamic stability between C-binding and N-binding complexes in the reaction of [1,2] carbon migration in N-heterocyclic carbene-coordinated transition metal complexes [56].

Very recently, some of us demonstrated a novel strategy to achieve thermodynamically and kinetically favorable activation of the C–F bond over the C–H bond dually driven by coordination and aromaticity (Fig. 4d). MCI values increase gradually along reaction coordinates, suggesting that aromaticity plays an important role in stabilizing the transition states and products during the reactions [57].

Aromaticity also plays a critical role in a bond shifting in [4n]annulene chemistry. Castro and co-workers found that the thermal *cis-trans* isomerization of [12]annulene involves a Möbius aromatic transition state (Fig. 4e) [58]. The reaction barrier for the isomerization of **57** to **60** was only 18.0 kcal mol^{−1}. The Möbius-twist transition state (**57-TS**) for this process is highly aromatic, which was supported

by a small ΔBL value (the variation between the longest and shortest C–C bonds in the annulene ring, 0.031 Å), a negative NICS(0) value (−13.9 ppm) and magnetic susceptibility exaltation (Λ, −43.8 cgs-ppm). This work represents a rare example of the Möbius aromatic transition state in the bond isomerization of [4n]annulenes.

The Möbius aromatic transition state was also proposed computationally in the [1,7]-hydrogen shift of 1,3,5-heptatriene by Jiao and Schleyer in 1993 [59]. In addition, Rzepa reported double-twist Möbius aromaticity in the transition state of a 10 electron electrocyclic reaction of a (Z,E,Z)-decapentaene [60]. In 2009, Mauksch and Tsogoeva proposed a Möbius aromatic transition state in an electrocyclic reaction with Möbius twisted topology [61]. As shown in Fig. 4f, the 12-electron transition states **61-TS** and 10-electron **62-TS** were aromatic according to the calculated negative NICS(0) values (−12.8 and −12.1 ppm, respectively). In addition, they extended this study to a system with a shorter carbon chain, that is, an 8-electron acyclic decapentaene dication **64** undergoes ring closure via a Möbius aromatic transition state **64-TS** (NICS(0) = −13.8 ppm) with a reaction barrier of 23.9 kcal mol^{−1}. In addition, a Craig–Möbius-like σ-aromatic transition state (NICS(0) = −19.4 ppm) was proposed in the Pd-catalyzed [π2s + π2s + σ2s + σ2s] pericyclic reaction, which was symmetry-allowed in the ground state due to the phase inversion introduced by *d* orbitals of the Pd atom (Fig. 4g) [62].

Aromatic transition state was also involved in the pericyclic reactions. For instance, the two triangles in the transition state (**68-TS**) for the rearrangement reaction of 1,2-dichloroethane are aromatic, as suggested by the larger negative NICS(0) values of −22.2 ppm (Fig. 4h) [63]. In addition, the 6MR transition state in the double-group transfer reaction (rearrangement of syn-sesquinorbornene) has also been demonstrated to be aromatic via the negative NICS value of −27.7 ppm (at the (3,+1) ring critical point of electron density) [64]. It should be noted that the products and reactants in this rearrangement process are non-aromatic. Interestingly, Algarra reported an unusual pericyclic reaction that involves an intermolecular S₃ transfer (Fig. 4h), which occurs via a concerted transition state featuring two five-membered C₂S₃ fused rings [65]. The calculated NICS at the (3,+1) ring critical points of electron density and ACID suggest that the two five-membered C₂S₃ rings are aromatic.

6. Antiaromaticity-destabilized reactants in reaction mechanisms

As antiaromaticity is a destabilized effect, antiaromatic reactants should exhibit higher reactivity than nonaromatic or aromatic reactants. With this idea in mind, some of us recently developed an antiaromaticity-promoted H₂ splitting by the combination of antiaromatic borole and aromatic pyridine into the cyclooctatetraene skeleton [66]. This system can be viewed as FLPs due to the geometric constraints. In the process of H₂ activation, breaking an antiaromatic boron-containing heterocycle will reduce the reaction barrier whereas reacting with aromatic boron-containing heterocycle will increase the reaction barrier (Fig. 5a). In contrast, for nonaromatic and aromatic B/N-substituted cyclooctatetraenes, the activation energies for H₂ splitting were moderately higher. Especially for the aromatic reactant, the reaction becomes both kinetically and thermodynamically unfavorable and the reaction barrier is as high as 36.1 kcal mol^{−1}. This study provides a novel strategy to design FLP systems for the activation of H₂ or other small molecules via antiaromaticity.

Fernández and Cabrera-Trujillo demonstrated that antiaromaticity can enhance the reactivity of FLPs for CO₂ and CS₂ activation [67]. For CO₂ and CS₂ activation (Fig. 5b), the activation barriers increased in the order of antiaromatic **78b** (5.8 and 8.3 kcal mol^{−1} for CO₂ and CS₂, respectively) < non-aromatic **78a** (7.5 and 13.6 kcal mol^{−1}). The calculated NICS(0) values for **78b**, **79b-TS** and **80b** decrease in the order of 14.0, 7.9 and 4.2 ppm for CO₂ activation with **78b**. In other words, along with the reaction coordinate, the transition state and product become less antiaromatic. A similar conclusion can be drawn for CS₂ activation. Obviously, the antiaromaticity of reactant plays a crucial role in the ac-

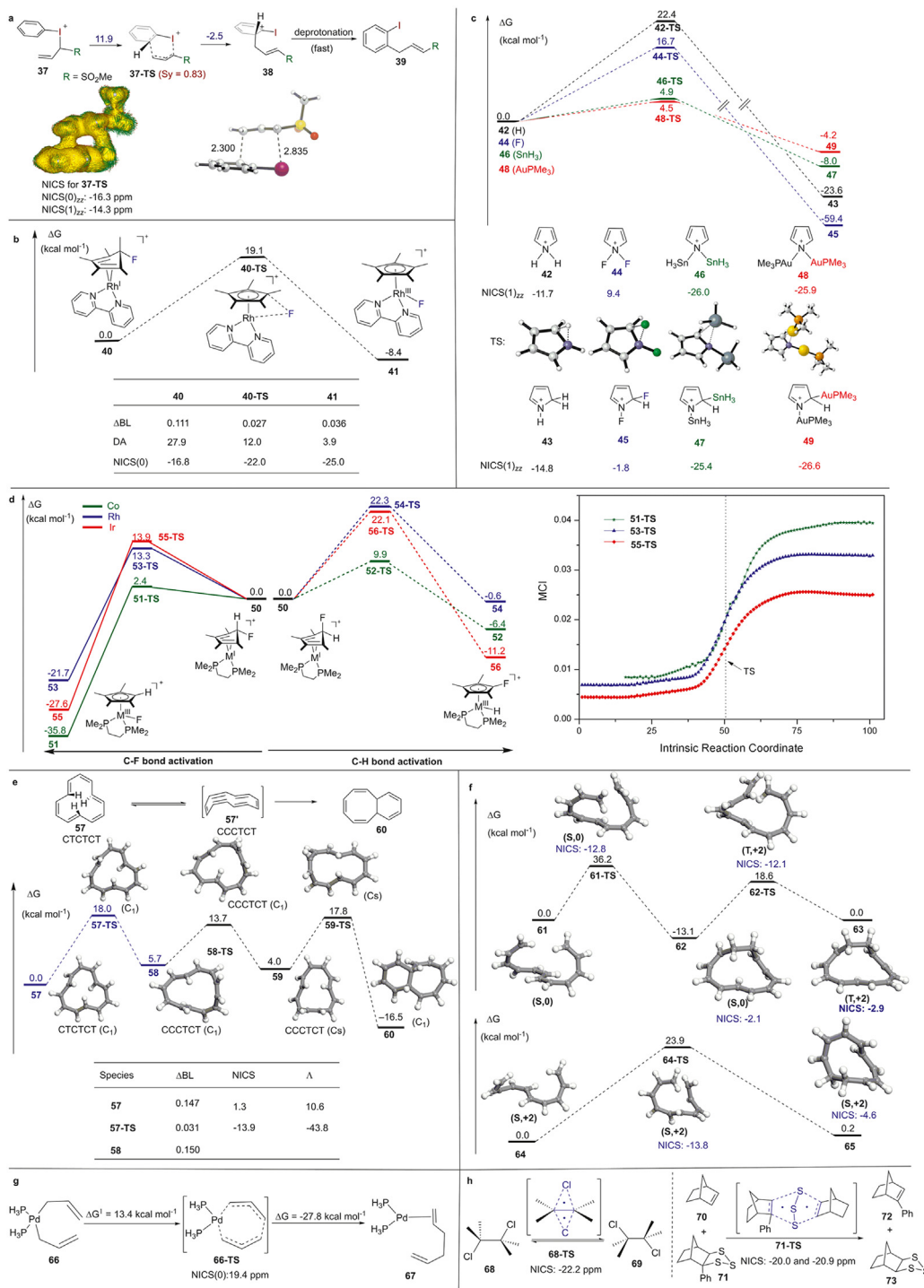


Fig. 4. Aromaticity-stabilized transition states in single bond activation. (a) DFT calculation of the “iodo-Claisen” rearrangement step. ACID plot (isovalue: 0.020 a.u.) along with the key distances (Å) and NICS (ppm) values [50]. Computational method, M06–2X/aug-cc-pVTZ-(PP)//M06–2X/def2-SVP. (b) Energy profiles for C–F bond activation by the Rh^I complex at the level of GD3-SMD (acetonitrile)-M06/6–311++G(d,p)(LanL2TZ(f))/B3LYP/6–31G(d,p)(LanL2DZ) [52]. The ΔBLs (Å), dihedral angles of the Cp* ring (DA) and NICS(0) values (ppm) were calculated at the level of B3LYP/6–311++G(d,p)(LanL2TZ(f)). (c) Gibbs energy profiles for the [1,5] shift of substituted pyrroliums [53]. Computational method, GD3-M06L/6–311++G(d,p)(ECPnMDF)/TPSS/6–311++G(d,p)(ECPnMDF). NICS(1)_{zz} value (in ppm) calculated at the level of TPSS/6–311++G(d,p)(ECPnMDF). (d) Gibbs energy profiles calculated of C–F and C–H bonds activation in different metal complexes; MCI values along the intrinsic reaction coordinate of C–F [57]. Computational method, at the level of SMD(acetonitrile)(U)B3LYP-D3/6–311++G(d,p)(LanL2TZ(f))/(U)B3LYP-D3/6–31G(d,p)(LanL2DZ). The ΔBLs (Å), dihedral angles of the Cp* ring (DA) and NICS(0) values (ppm) were calculated at the level of B3LYP/6–311++G(d,p)(LanL2TZ(f)). (e) Gibbs energy profile for the isomerization of [12]annulene. C and T represent *cis* and *trans* configurations, respectively [58]. Computational method, CCSD(T)/cc-pVDZ//BH&HLYP/6–311+G(d,p). NICS(0) (ppm) and Λ (cgs-ppm) computed at the B3LYP/6–311+G(d,p)//BH&HLYP/6–311+G(d,p). (f) Gibbs energy profile for the thermal electrocyclic reaction [61]. Computational method for C₁₂H₁₄ and C₁₀H₁₂ species at the level of CCSD(T)/6–31G//B3LYP/6–31G(d) and CCSD(T)/6–31G(d)//B3LYP/6–31G(d), respectively. NICS values calculated for the center of mass (in ppm) at the B3LYP/6–31G(d) level. Multiplicity (Singlet = S, Triplet = T) and charge are given in black parentheses. (g) Pd-catalyzed [π2s + π2s + σ2s + σ2s] pericyclic reaction [62]. Computational method, PBE0-D3(BJ)/NEVPT2. (h) Transition state structures and NICS (ppm) for the transition states of rearrangement of 1,2-dichloroethane and syn-sesquibornene, as well as the S3 transfer reaction [63].

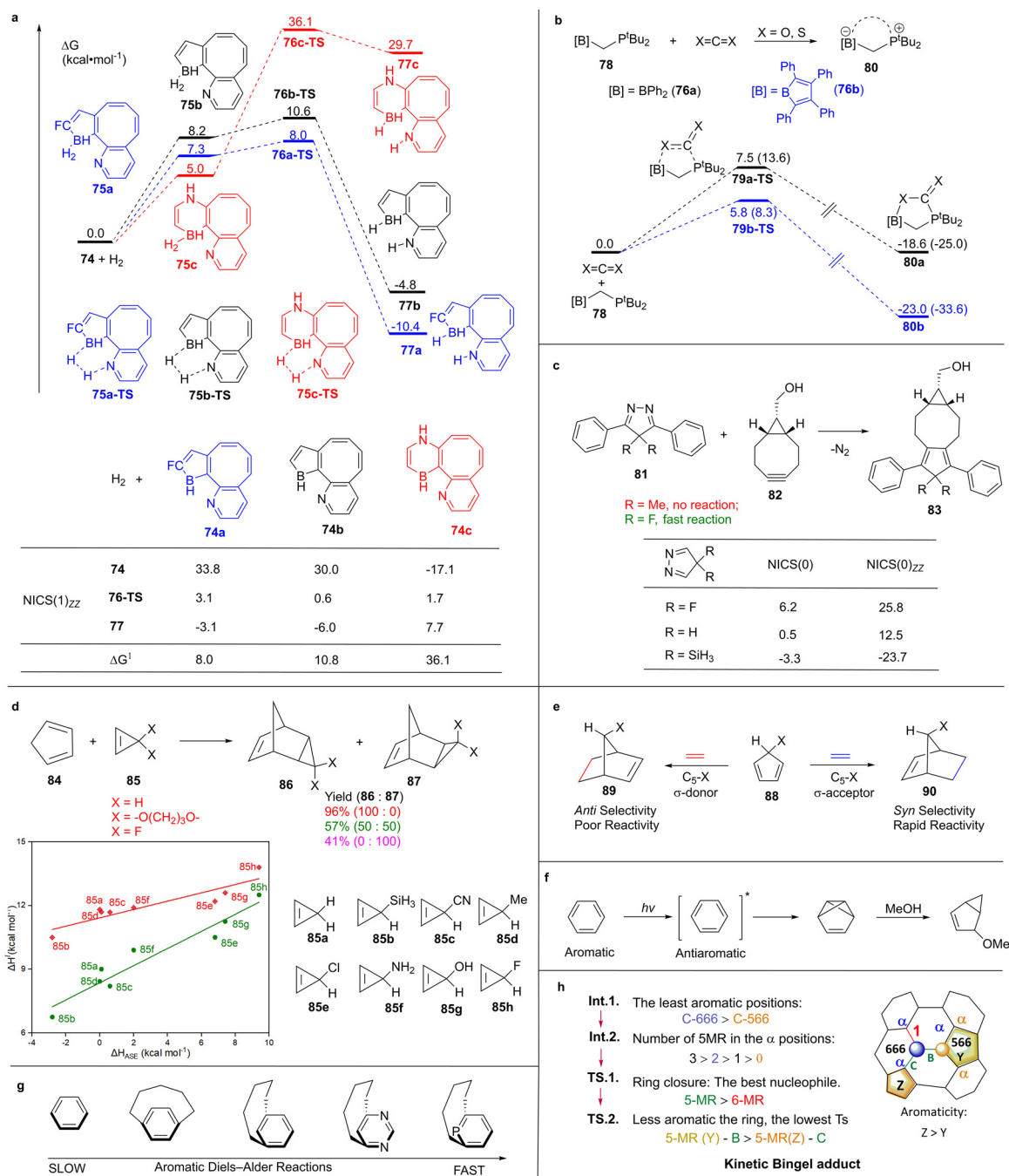


Fig. 5. Antiaromaticity-destabilized or aromaticity-reduced reactants in reaction mechanisms. (a) Gibbs energy profile for H₂ activation by a boron-containing heterocycle [66]. Computational method, ωB97XD/cc-pVTZ. NICS(1)_{zz} values (in ppm) computed at the B3LYP/6-311G(d) level. (b) FLP-mediated CO₂ and CS₂ (in parentheses) activations [67]. Relative energies (in kcal mol⁻¹) obtained at the PCM(toluene)-M06-2X/def2-TZVPP//M06-2X/def2-SVP level of theory. (c) Diels–Alder reaction between pyrazole and cyclic alkyne. Hyper-conjugative antiaromaticity induced by fluorination accelerates the reactivity [69]. (d) Diels–Alder reactions between cyclopentadiene and substituted cyclopropenes [71]. Correlation of the endo (green) and exo (red) Diels–Alder reactions activation enthalpy (ΔH[‡]) with hyperconjugative aromatic stabilization enthalpy (ΔH_{ASE}) of butadiene with cyclopropenes. The hyperconjugative aromaticity or antiaromaticity of the cyclopropenes has a great effect on the stereoselectivity. (e) *Syn* and *Anti* Diels–Alder cycloaddition between cyclopentadiene and ethylene [72]. The stereoselectivities for this reaction were also controlled by hyperconjugative (anti)aromaticity. (f) Excited-state antiaromaticity triggers nucleophilic addition of MeOH to benzene [74]. (g) Aromatic Diels–Alder reactions of benzene tuned by geometric distortion and/or heteroatom substitution [76]. (h) Predictive aromaticity-based criteria (PAC) for the Bingel–Hirsch addition to isolated pentagon rule endohedral metallofullerenes [78,79].

tivation of CO₂ and CS₂, and along the reaction coordinate, the antiaromatic character was mitigated, thus reducing the energy barrier. Moreover, this antiaromatic reactant-promoted activation strategy can be extended to other small molecule activations, including H₂, CH₄, SiH₄ and acetylene [67]. In contrast, the author recently reported aromaticity-enhance reactivity of geminal FLP [68].

Subsequently, Houk, Raines and co-workers investigated the Diels–Alder reaction between 4,4-difluoro-3,5-diphenyl-4H-pyrazole and endo-bicyclo[6.1.0]non-4-yne both experimentally and theoretically (Fig. 5c) [69]. They found that the 4,4-dimethyl-3,5-diphenyl-4H-pyrazole was inactive in this reaction and thus the hyperconjugative antiaromaticity induced by fluorination of the cyclopentadiene en-

hanced the reactivity. Further studies show that the NICS(0) values for the unsubstituted 4*H*-pyrazole and the fluorinated one were 0.5 ppm and 6.2 ppm, respectively, whereas that of silylated 4*H*-pyrazole was –3.3 ppm, suggesting the hyperconjugative antiaromaticity induced by fluorination of 4*H*-pyrazole. In addition, Harper and co-workers found that the antiaromaticity dramatically affects the rate of the acid catalyzed methanolysis of a series of substituted benzhydrols and fluorenols even though they undergo the same reaction mechanism [70].

Houk and Lewandowski also examined the stereoselectivities for the Diels–Alder cycloaddition reactions between the substituted cyclopropenes and cyclopentadiene (Fig. 5d) [71]. They found that the hyperconjugative aromaticity or antiaromaticity of the cyclopropenes has a great effect on the reactivity. For example, the *endo* stereoselectivity and reactivity were increased by introducing a σ -donor substituent at the C3 position due to antiaromatic character of cyclopropene ring caused by pseudo four electrons, whereas the acceptor substituents had the opposite effect. The antiaromatic character was confirmed by the negative aromatic stabilization enthalpy (e.g., –2.8 kcal mol^{–1} for 3-silylcyclopropene). Therefore, σ -donors destabilize the antiaromatic cyclopropene ring and the reactivity is enhanced.

In addition, they also investigated the stereoselectivities for the Diels–Alder cycloadditions of 5-substituted cyclopentadienes [72]. Result shows that the substituent X at the C5 atom influences the stereoselectivities of the reaction (Fig. 5e). When X is a σ -acceptor, cyclopentadiene prefers to distort in the opposite direction to minimize the destabilizing effect of hyperconjugative antiaromaticity, which was also confirmed by the negative aromatic stabilization enthalpy (e.g., –3.4 kcal mol^{–1} for F-substituted cyclopentadiene). In contrast, cyclopentadiene with a σ -donor prefers to transform into an envelope conformation to maximize the hyperconjugative effect. For example, the Diels–Alder cycloaddition reaction of 5-acetoxycyclopentadiene with ethylene exclusively forms the *syn* adduct [73].

Benzene is the most typical aromatic molecule in the electronic ground state, however, it is antiaromatic in the lowest S₁ excited state according to Baird's rule. Therefore, the antiaromatic benzene in the excited state could be activated. Recently, Ottosson and co-workers reported that an excited-state antiaromaticity triggers nucleophilic addition of benzene to synthesize a series of substituted bicyclo[3.1.0]hex-2-enes (Fig. 5f) [74]. In addition, the excited-state antiaromaticity triggered reaction could be also extended to other 6 π -electron heterocycles, such as silabenzene and pyridinium, leading to the formation of three-dimensional molecular scaffolds. The excited-state aromaticity also affects the ring inversion of a pair of molecules with thiophene-fused chiral [4*n*]annulenes [75].

In addition to antiaromaticity-destabilized the reactants, if the aromaticity in the reactant was reduced or destroyed, the reaction could also be accelerated. For instance, Bickelhaupt and co-workers found that the distorted aromatic core or heteroatom-substituted aromatic ring have lower activation barriers in aromatic Diels–Alder reactions than their planar aromatic analogues, which is probably due to the aromaticity of the reactants being partially broken due to the structural distortion (Fig. 5g) [76]. In addition, Ullmann and co-workers reported that the Tungsten-Containing Benzoyl-CoA Reductase could degrade the aromatic compounds as the W(IV) center lowers the barrier for breaking the aromaticity of the substrates [77].

Some of us found that the different aromaticities of the 5MRs and 6MRs of fullerene C₆₀ have a significant impact on the energy barriers and regioselectivity of Diels–Alder, 1,3-dipolar, and carbene cycloadditions, which can take place over the [6,6] and [5,6]-bonds of C₆₀ [78,79]. For example, the aromaticity of the 6-MRs in C₆₀ decreases when the negative charge [78] or the spin [79] of C₆₀ increases, whereas the 5MRs become more aromatic. Therefore, for the Diels–Alder reaction between negatively charged or high-spin C₆₀ and cyclopentadiene, addition to a [5,6] bond, which breaks the aromaticity of three 6MRs and only one 5MR, becomes more favorable than an addition to a [6,6] bond, which breaks the aromaticity of two 6-MRs and two 5-MRs (Fig. 5h).

Moreover, predictive aromaticity criteria was developed for the regioselectivity Bingel–Hirsch (BH) addition to isolated pentagon rule (IPR) endohedral metallofullerenes (EMFs) [80]. The BH addition is a cyclopropanation reaction where a fullerene and diethyl bromomalonate in the presence of a strong base such as 1,8-diazabicycloundec-7-ene (DBU) react to produce a methanofullerene or a fulleroid. In the first step of the reaction mechanism, the base abstracts the acidic proton of the malonate derivative to generate a carbanion or enolate. Then this carbanion nucleophilically attacks the fullerene, thus generating a new carbanion with charge localized at the cage. In the final step, bromide is displaced in a nucleophilic substitution S_N2 reaction causing an intramolecular three-membered ring (3MR) closure. The regioselectivity patterns for the BH addition on IPR EMFs can be predicted using a set of aromaticity-based criteria, the so-called Predictive Aromaticity Criteria (PAC) (Fig. 5h). The PAC criteria identify the lowest energy intermediates and transition states for a given IPR EMF from the initial fullerene structure. The most aromatic (and therefore lowest in energy) intermediates lead to the lowest activation barriers for the BH addition. Finally, Chen and co-workers found that the aromaticity or antiaromaticity of the transition metal macrocyclic complexes could have a remarkable effect on their oxygen reduction reaction activity [81]. Macrocycles with antiaromaticity could enhance the activity of metal centers.

7. Aromaticity-stabilized products in reaction mechanisms

Aromaticity has also a significant effect on polymetalated species. By a combination of experiments and DFT calculations, some of us found that the indolyl 5MR in complex **93**, containing two gem-diaurated tetrahedral carbon atoms, exhibits extended hyperconjugative aromaticity with two sp³ hybridized carbon atoms (Fig. 6a) [82]. Based on the calculated Δ BLs and negative NICS(1)_{zzz} values, complex **93** exhibits higher delocalization and more remarkable aromaticity than **92**. Due to the stronger electron delocalization in indolyl 5MR of **93**, the lone pair electrons of the N atom are more involved in the delocalization, which reduces the electron density of the N–Au bond and thus weakens it. The aromaticity in penta-aurated indolium **93** shows an extended electron conjugation due to dual hyperconjugation. Such a difference on aromaticity accounts for a facile protodeauration for **93**.

Braunschweig, Lin and co-workers reported the reaction of boroles with alkynes to generate boranorbornadiene, borepin and/or boracyclohexadiene, respectively, by DFT studies (Fig. 6b) [83]. Among them, they found that the formation of borepin by the reaction of borafullerene with alkynes was due to the propensity to maintain its aromaticity, with a reaction barrier and reaction energy of 22.2 and –21.5 kcal mol^{–1}, respectively. Boranorbornadiene **97** was not observed in this reaction due to the unfavorable dearomatization.

Wegner and co-workers reported the selective functionalization of CO₂ by a bidentate borohydride Li₂[1,2-C₆H₄(BH₃)₂] catalyst, in which CO₂ was transformed to either methane or methanol under Et₃SiH/B(C₆F₅)₃ or pinacolborane as reducing agents [84]. They found that the aromaticity in the seven-membered ring plays an important role in the stabilization of the intermediate (1,3-dioxo-4,7-diborepine heterocycle) in this bidentate interaction, which was confirmed by the good planarity of the entire ring of **101a** in the X-ray structure (Fig. 6c). This study again demonstrates that aromaticity could play an important role in the transition-metal-free activation of small molecules.

Some of us predicted via DFT calculations that replacing the highly active methyleneborane by tri-coordinated boron species can be also used for N₂ fixation (Fig. 6d) [85]. The Gibbs activation energy ($\Delta G^{0\ddagger}$) and overall Gibbs reaction energy for N₂ activation via NHC-borole-based FLPs were 21.2 and –61.7 kcal mol^{–1}, respectively, indicating that the N₂ activation could become thermodynamically favorable and kinetically feasible. Further study shows that aromaticity plays a crucial role in this process. The newly formed 5MR (A) and 6MR (B) in product **104** possess significantly negative NICS(1)_{zzz} values of –19.2 and –17.4 ppm, respectively, suggesting aromaticity in both rings.

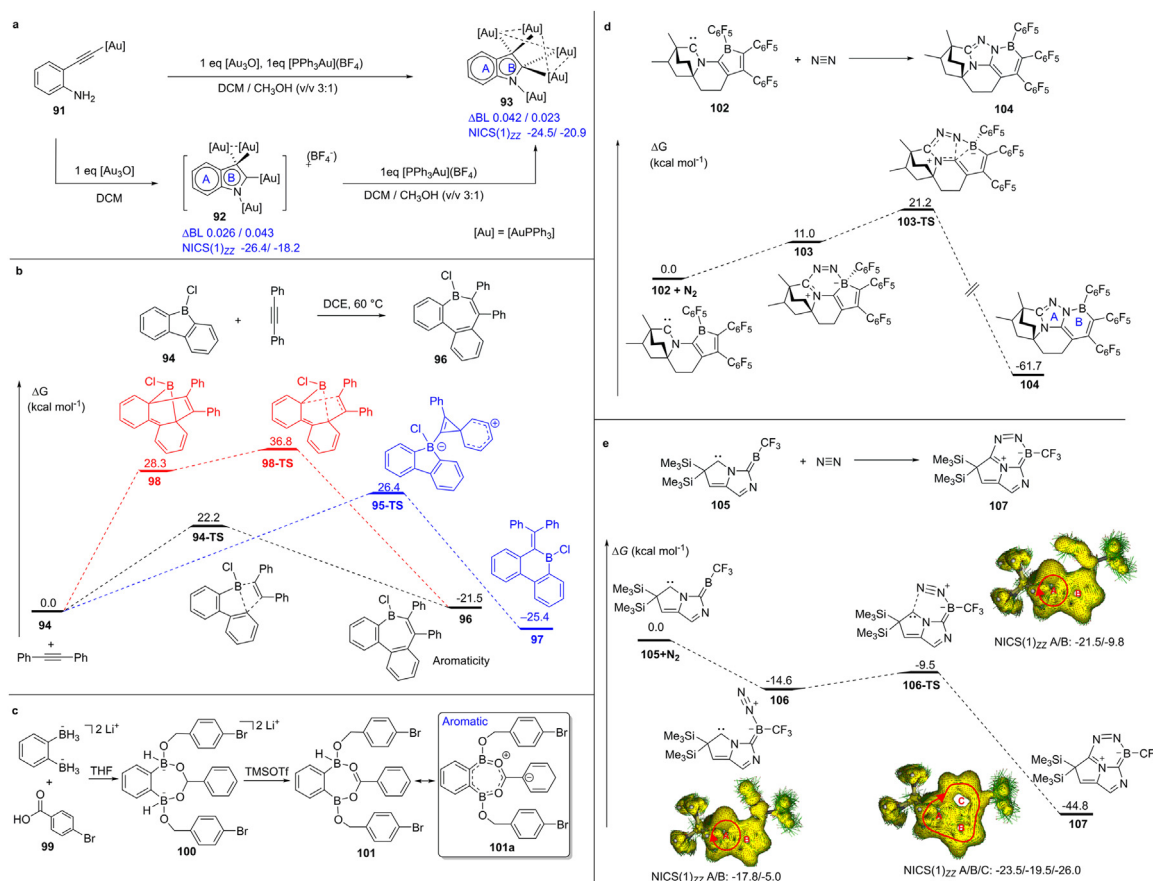


Fig. 6. Aromaticity-stabilized products in reaction mechanisms. (a) Synthetic and protodeauration of polyaurated indolium complexes [82]. Computational method, TPSS/6–31G(d)(ECP60MDF). (b) Gibbs energy profiles for borenium formation by the reaction of borafluorene reacted with alkynes [83]. Computational method, PCM(dichloromethane)-D3-M05–2X/6–311++G(d,p)//M05–2X/6–31G(d) for C, H, B, and F, 6–311++G(d,p) for Cl, and LanL2DZ for Si. (c) Aromatic intermediate 101a in CO_2 reduction [84]. (d) Gibbs energy profile for the N_2 activation by NHC-borole-based FLP [85]. Computational method, $\omega\text{B97XD/cc-pVTZ}/\omega\text{B97XD/cc-pVDZ}$. (e) Gibbs energy profile for the N_2 activation by FLPs [86].

Very recently, some of us systematically investigated an experimentally viable FLP containing two moieties (methyleneborane and carbene) could be effective for the N_2 activation in a thermodynamically and kinetically favorable manner (Fig. 6e) [86]. Aromaticity is found to play a crucial role in stabilization of the product. NICS(1)_{zz} values and ACID plots for ring A show comparable hyperconjugative aromaticity due to pseudo six π -electrons in the 5MR. The NICS(1)_{zz} values in the rings A, B, and C in product 107 are -23.5 , -19.5 and -26.0 ppm, respectively, indicating that aromaticity plays a crucial role in stabilization of the product. This study further highlights great potential of metal-free FLPs for N_2 activation.

Metalla-aromatics exhibit unique properties due to the metal d orbital being involved in the conjugated structures [87–91]. The aromaticity in the final product plays an important role in their successful syntheses and characterization. For instance, in 2013, Xia, Zhu and co-workers reported an unusual complex (metallapentalyne) with a metal-carbon triple bond in a 5MR, which was synthesized by the reaction of complex 108 with alkyne (Fig. 7a) [92]. Metallapentalyne 109 exhibits excellent stability although it contains a particularly small carbyne bond angle (129.5°). The aromaticity in the product was confirmed by the negative NICS(0)_{zz} values for the two fused 5MRs (-11.1 and -10.8 ppm, respectively) and the negative ISE values (around $-23 \text{ kcal mol}^{-1}$). In addition, by the reaction of complex 108 with allenylboronic acid pinacol ester, metallapentalene complex 110 with a metallacyclopentene unit was formed (Fig. 7a) [93]. DFT studies show that the NICS(0) value for the 3MR was -40.6 ppm, which was mainly attributed to the σ orbitals (-34.8 ppm). Therefore, the σ -aromaticity was first suggested to be

dominant in an unsaturated 3MR. The σ -aromaticity in the 3MR and the π -aromaticity in the two 5MRs were further confirmed by ACID analysis.

Subsequently, Xia and co-workers reported the formation of a metal-bridged tricyclic aromatic system by the nucleophilic addition of an aryl nucleophile with osmapentalyne followed by intramolecular C–H activation (Fig. 7b) [94]. DFT calculations show that the NICS(1)_{zz} values for the three 5MRs around the osmium center are distinctly negative. The aromaticity-driven products were further confirmed by the planarity, high stability, down-field proton chemical shifts, and calculated ISE values in the three 5MRs of complexes 112 and 113. In addition, Xia group also reported electrophilic aromatic substitution (EAS) reactions of Craig-Möbius aromatics (osmapentalenes, fused osmapentalenes), in which the highly reactive nature of osmapentalene makes it susceptible to electrophilic attack by halogens [95].

Aromaticity-driven reactions were also observed in the reaction of complex 111 with nitriles. Xia and co-workers found that the $\text{C}\equiv\text{N}$ triple bond in two molecules of nitriles could react with the metal-carbon triple bond in 111 via a [2+2+2] cycloaddition (Fig. 7c) [96]. The [2+2+2] cycloaddition reaction [97] gives a metallapyrazine unit first, followed by oxidative aromatization in the presence of hypervalent iodine and acid, leading to the formation of a metallapentalenopyrazine derivative. Product 115 has the character of equalized bond lengths and downshifted proton. The clockwise ring currents of the ACID plot, negative ISE values of rings A and B measured with two different reactions (-23.9 and $-26.3 \text{ kcal mol}^{-1}$) and negative NICS(1)_{zz} values (for ring A: -26.9 ppm, B: -15.3 ppm, and C: -15.6 ppm) further verify the aromaticity in metallapentalenopyrazine [96].

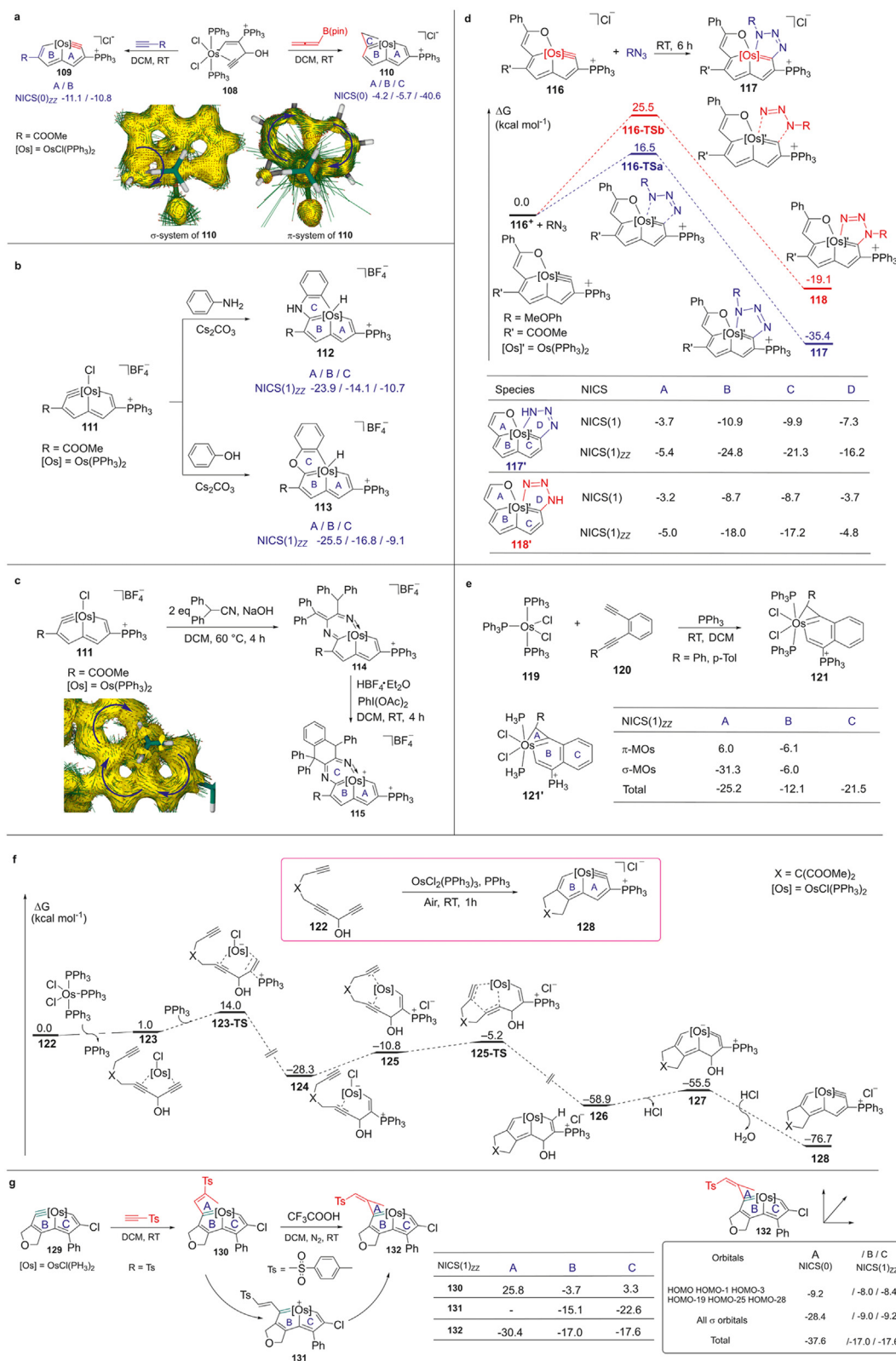


Fig. 7. Metalla-aromaticity-stabilized products in reaction mechanisms. (a) Syntheses and aromaticity evaluation of aromatic metallapentalyne and metal-lapentalene derivatives [92,93]. (b) Syntheses and aromaticity evaluation of polycyclic metallaromatics [94]. Computational method, B3LYP/6-311++G(d,p). NICS values given in ppm. (c) Aromaticity-promoted [2+2+2] cycloaddition reaction of a metal-carbyne complex with nitriles [96]. Computational method, B3LYP/6-311++G(d,p)(LanL2DZ). (d) Gibbs energy profiles for cycloaddition reactions of 4-anisyl azide and osmapentalyne [98]. Computational method, PCM(dichloromethane)-B3LYP-D3BJ/6-311++G(d,p)(LanL2TZ). Selected bond lengths given in Å. The NICS(1)_{zz} values of metal-bridgehead tetracyclic complexes. Computational method, B3LYP/6-311++G(d,p)(LanL2TZ). [Os]' = Os(PH₃)₂. (e) σ -aromaticity promoted the C≡C triple bond activation [99]. Computational method, B3LYP/6-311++G(d,p)(LanL2DZ). (f) Gibbs energy profiles of the aromaticity-driven cyclization reaction of the multiyne chain with OsCl₂(PPh₃)₃ [100]. Computational method, PCM(dichloromethane)-TPSS/6-31G(d)(SDD)//B3LYP/6-31G(d)(SDD). (g) Ring contraction of metallacyclobutadiene to metallacyclopentadiene driven by π - and σ -Aromaticity Relay [102]. Computational method, PCM(dichloromethane)-TPSS/6-31G(d)(SDD)//B3LYP/6-31G(d)(SDD).

Recently, Xia groups reported a metalla-click reaction between metal-carbyne and azides, in which a metal center shared by four aromatic rings was formed with remarkable regioselectivity [98]. Mechanistic studies showed that the formation of 1,4 metallatriazole regioisomer **117** was both kinetically and thermodynamically favorable (Fig. 7d). The NICS(1)_{zz} values of metallatriazole unit in the **117'** (−16.2 ppm) were more negative than those in **118'** (−4.8 ppm), indicating that the aromaticity plays a dominant role in stabilizing 1,4 metallatriazole rather than 1,5 metallatriazole regioisomers.

Chen and co-workers reported the first example of cyclopropametallaphthalenes [99], in which the σ -aromaticity in the osmacyclopentene ring could be used to explain the stability of the product (Fig. 7e). The aromaticity in complex **121** was documented by the negative NICS value at the center of the osmacyclopentene ring from all the σ -MOs (NICS(1)_{zz} = −31.3 ppm) by canonical molecular orbital NICS calculations. Moreover, the calculated ISE value and ACID are in line with the NICS value, further confirming the σ -aromaticity in the 3MR.

Actually, metallapentalene can be also synthesized by a one-pot reaction of multiynes with OsCl₂(PPh₃)₃, which is also an aromaticity-driven process [100]. The reaction barrier for the rate-determining step is 23.1 kcal mol^{−1} (Fig. 7f). The negative NICS(1)_{zz} values (−17.3 and −14.3 ppm in A and B rings, respectively) and positive aromatic stabilization energy (29.5 kcal mol^{−1}) in complex **128** further confirmed that the pericyclic reaction was an aromaticity-driven process. In addition, an 11-center-12-electron d_π-p_π conjugated α -metallapentalenofurans was also proven to be a Möbius aromaticity promoted product, which was constructed by the reactions of osmapentalene with terminal aryl alkynes in the presence of H₂O [101].

Xia groups reported an unusual acid-induced ring contraction of metallacyclobutadiene to metallacyclopentene via a ring-opening-reclosing process very recently [102]. The results of theoretical calculations indicate that aromaticity plays a major role in this reaction (Fig. 7g). The ring-opening of A ring (NICS(1)_{zz}, 25.8 ppm) in **130** to form **131** (NICS(1)_{zz}, −15.1 and −22.6 ppm in B and C rings, respectively) involves the release of antiaromaticity accompanied by the strengthening of the π -aromaticity in osmapentalene and can be considered as a π -aromaticity-driven process. Then, the ring-reclosing process from **131** to **132** (NICS(1)_{zz} for ring A: −30.4 ppm, B: −17.0 ppm, and C: −17.6 ppm) further expands the aromaticity system of the metallacycles with newly formed σ -aromaticity, which are supported by the results of canonical molecular orbital (CMO) NICS analysis for the 3MR in complex **132**. The total diamagnetic contribution of the NICS(0) value for the 3MR from the six occupied π molecular orbitals (HOMO, HOMO-1, HOMO-3, HOMO-19, HOMO-25, and HOMO-28) was −9.2 ppm, whereas the NICS(0) value contributed by all the σ -orbitals (−28.4 ppm) was much more negative, indicating that σ -aromaticity is dominant in the 3MR and is the major contribution to aromaticity in the 3MR of **132**.

8. Limitation

However, there are still some limitations for the application of aromaticity in the small-molecule activation. First, cyclic structures are required for a reactant, intermediate, transition state or product in a given reaction as aromaticity is used to describe the mobility of π electrons in a cyclic species, limiting the types of reactants or products to some extent. Secondly, although antiaromaticity in a reactant might promote a reaction, preparation of highly reactive reactants demands harsh synthetic and storage conditions. Thirdly, some aromaticity indices such as HOMA or FLU cannot be applied along a reaction coordinate of a given cycloaddition and others, like NICS, are not reliable in points of space close to transition metals [103]. Fourthly, the utilization of the strategy by improving the aromaticity of the transition state to reduce a reaction barrier still remains a major challenge as both aromaticity and transition state cannot be probed experimentally. It should be also noted that the interaction involving bond cleavage and formation in most transition states is particularly weak. It is no wonder that these transition states

in some classical pseudocyclic reactions were considered to be nonaromatic due to lack of adequate electron delocalization when benzene is used as a reference [104].

9. Conclusion and outlook

Small molecule activation and functionalization have been widely applied to construct value-added products, attracting great attention in the field of synthetic chemistry. On the other hand, aromaticity is one of the most important and fundamental concepts that has been frequently discussed. Here, we devote ourselves to a summary of aromaticity as a key factor in the reaction mechanisms. The strategy can be mainly classified into two modes: the first one is to reduce the antiaromaticity of the reactant whereas the second one is to enable the aromaticity in a transition state or an intermediate or a product. Hyperconjugative antiaromaticity is usually employed in the first mode by tuning the substituents. In addition, aromaticity gained or antiaromaticity reduced along the reaction coordinate is the most common strategy, which is widely used by experimental and theoretical chemists. Note that releasing antiaromaticity in an excited arene is another less developed strategy [105] to promote a reaction. Developing metalla-aromatics as a catalyst in organic synthesis could be another direction and some examples have been demonstrated to display robust catalytic activity for metathesis [106] and selective difunctionalization of unactivated aliphatic alkenes [107]. With the rapid development of computational resource, quantum chemical calculations will make significant contributions to aromaticity-driven reactions by rationalizing the proposed reaction mechanisms and predicting new and novel reactions or catalysts via theoretical design and computational screening for experimental validation.

Author contributions

Q.Z. D.C. and S.C. drafted the paper. J.Z., M.S., and L.Z. refined the text. All authors discussed the results and contributed to the preparation of the final manuscript.

Declaration of competing interest

The authors declare that they have no conflicts of interest in this work.

Acknowledgments

Financial support by the National Natural Science Foundation of China (22073079, 22025105 and 21873079), the Ministry of Education of China (H20200504) and the Top-Notch Young Talents Program of China is gratefully acknowledged. M.S. thanks the Ministerio de Ciencia e Innovación of Spain (project PID2020-113711GB-I00) and the Generalitat de Catalunya (project 2017SGR39).

References

- [1] Y. Tian, G. Zhu, Porous aromatic frameworks (PAFs), *Chem. Rev.* **120** (2020) 8934–8986.
- [2] I. Fernández, *Aromaticity: Modern Methods and Applications*, 1st ed., Elsevier, 2021.
- [3] E. Matito, J. Poater, M. Solà, et al., *Aromaticity and chemical reactivity*, in: P.K. Chattaraj (Ed.), *Chemical Reactivity Theory: A Density Functional View*, CRC Press, Boca Raton, 2009, pp. 419–438.
- [4] H. Zimmerman, Möbius-Hückel concept in organic chemistry. Application of organic molecules and reactions, *Acc. Chem. Res.* **4** (1971) 272–280.
- [5] K.N. Houk, F. Liu, Z. Yang, et al., Evolution of the Diels–Alder reaction mechanism since the 1930s: Woodward, Houk with Woodward, and the influence of computational chemistry on understanding cycloadditions, *Angew. Chem. Int. Ed.* **60** (2020) 12660–12681.
- [6] M.G. Evans, The activation energies of reactions involving conjugated systems, *Trans. Faraday Soc.* **35** (1939) 824–834.
- [7] P.v.R. Schleyer, J.I. Wu, F.P. Cossío, et al., Aromaticity in transition structures, *Chem. Soc. Rev.* **43** (2014) 4909–4921.
- [8] N.C. Baird, Quantum organic photochemistry. II. Resonance and aromaticity in the lowest ³ $\pi\pi^*$ state of cyclic hydrocarbons, *J. Am. Chem. Soc.* **94** (1972) 4941–4948.

- [9] H. Otosson, Exciting excited-state aromaticity, *Nat. Chem.* 4 (2012) 969–971.
- [10] H. Otosson, Durbjee B, M. Solà, Excited-state aromaticity and antiaromaticity special issue, *J. Phys. Org. Chem.* 36 (2023) e4468.
- [11] M. Rosenberg, C. Dahlstrand, K. Kilså, et al., Excited state aromaticity and antiaromaticity: opportunities for photophysical and photochemical rationalizations, *Chem. Rev.* 114 (2014) 5379–5425.
- [12] J. Yan, T. Slanina, J. Bergman, et al., Photochemistry driven by excited-state aromaticity gain or antiaromaticity relief, *Chem. Eur. J.* (2023) e202203748.
- [13] S. Shostak, W. Park, J. Oh, et al., Ultrafast excited state aromatization in dihydroazulene, *J. Am. Chem. Soc.* 145 (2023) 1638–1648.
- [14] L.J. Karas, C.-H. Wu, J.I. Wu, Barrier-lowering effects of Baird antiaromaticity in photoinduced proton-coupled electron transfer (PCET) reactions, *J. Am. Chem. Soc.* 143 (2021) 17970–17974.
- [15] B. Oruganti, P.P. Kalapos, V. Bhargav, et al., Photoinduced changes in aromaticity facilitate electrocyclicization of dithienylbenzene switches, *J. Am. Chem. Soc.* 142 (2020) 13941–13953.
- [16] O.E. Bakouri, J.R. Smith, H. Otosson, Strategies for design of potential singlet fission chromophores utilizing a combination of ground-state and excited-state aromaticity rules, *J. Am. Chem. Soc.* 142 (2020) 5602–5617.
- [17] Y.M. Sung, J. Oh, W.-Y. Cha, et al., Control and switching of aromaticity in various all-aza-expanded porphyrins: spectroscopic and theoretical analyses, *Chem. Rev.* 117 (2017) 2257–2312.
- [18] Y. Su, R. Kinjo, Small molecule activation by boron-containing heterocycles, *Chem. Soc. Rev.* 48 (2019) 3613–3659.
- [19] R. Herges, Topology in chemistry: designing Möbius molecules, *Chem. Rev.* 106 (2006) 4820–4842.
- [20] G.C. Welch, R.R.S. Juan, J.D. Masuda, et al., Reversible, metal-free hydrogen activation, *Science* 314 (2006) 1124–1126.
- [21] A. Brand, W. Uhl, Sterically constrained bicyclic phosphines: a class of fascinating compounds suitable for application in small molecule activation and coordination chemistry, *Chem. Eur. J.* 25 (2019) 1391–1404.
- [22] P.P. Power, Interaction of multiple bonded and unsaturated heavier main group compounds with hydrogen, ammonia, olefins, and related molecules, *Acc. Chem. Res.* 44 (2011) 627–637.
- [23] M. Soleilhavoup, G. Bertrand, Cyclic(alkyl)(amino)carbenes (CAACs): stable carbenes on the rise, *Acc. Chem. Res.* 48 (2015) 256–266.
- [24] N. Martín, L.T. Scott, Challenges in aromaticity: 150 years after Kekulé's benzene, *Chem. Soc. Rev.* 44 (2015) 6397–6400.
- [25] M. Solà, Why aromaticity is a suspicious concept? Why? *Front. Chem.* 5 (2017) 22.
- [26] J. Zhu, Open questions on aromaticity in organometallics, *Commun. Chem.* 3 (2020) 161.
- [27] G. Merino, M. Solà, I. Fernández, et al., Aromaticity: Quo Vadis, *Chem. Sci.* 14 (2023) 5569–5576.
- [28] D.W. Szczepaniak, M. Solà, M. Andrzejak, et al., The role of the long-range exchange corrections in the description of electron delocalization in aromatic species, *J. Comput. Chem.* 38 (2017) 1640–1654.
- [29] D.W. Szczepaniak, M. Andrzejak, K. Dydach, et al., A uniform approach to the description of multicenter bonding, *Phys. Chem. Chem. Phys.* 16 (2014) 20514–20523.
- [30] F. Feixas, E. Matito, J. Poater, et al., Quantifying aromaticity with electron delocalisation measures, *Chem. Soc. Rev.* 44 (2015) 6434–6451.
- [31] Z.-F. Chen, C.S. Wannere, C. Corminboeuf, et al., *Chem. Rev.* 105 (2005) 3842–3888.
- [32] S. Klod, E. Kleinpeter, Ab initio calculation of the anisotropy effect of multiple bonds and the ring current effect of arenes—application in conformational and configurational analysis, *J. Chem. Soc., Perkin Trans. 2* (2001) 1893–1898.
- [33] D. Geuenich, K. Hess, K. Köhler, et al., Anisotropy of the induced current density (ACID), a general method to quantify and visualize electronic delocalization, *Chem. Rev.* 105 (2005) 3758–3772.
- [34] H. Fliegl, S. Taubert, O. Lehtonen, et al., The gauge including magnetically induced current method, *Phys. Chem. Chem. Phys.* 13 (2011) 20500–20518.
- [35] C. Foroutan-Nejad, J. Vicha, A. Ghosh, Relativity or aromaticity? A first-principles perspective of chemical shifts in osmabenzene and osmapentalene derivatives, *Phys. Chem. Chem. Phys.* 22 (2020) 10863–10869.
- [36] T.M. Krygowski, Crystallographic studies of inter- and intramolecular interactions reflected in aromatic character of π -electron systems, *J. Chem. Inf. Comput. Sci.* 33 (1993) 70–78.
- [37] J. Zhu, K. An, P.V.R. Schleyer, Evaluation of triplet aromaticity by the isomerization stabilization energy, *Org. Lett.* 15 (2013) 2442–2445.
- [38] D. Singh, W.R. Buratto, J.F. Torres, et al., Activation of dinitrogen by polynuclear metal complexes, *Chem. Rev.* 120 (2020) 5517–5581.
- [39] M.-A. Légaré, G. Bélanger-Chabot, R.D. Dewhurst, et al., Nitrogen fixation and reduction at boron, *Science* 359 (2018) 896–900.
- [40] M.-A. Légaré, G. Bélanger-Chabot, M. Rang, et al., One-pot, room-temperature conversion of dinitrogen to ammonium chloride at a main-group element, *Nat. Chem.* 12 (2020) 1076–1080.
- [41] J. Zhu, Rational design of a carbon-boron frustrated Lewis pair for metal-free dinitrogen activation, *Chem. Asian J.* 14 (2019) 1413–1417.
- [42] Z. Xi, K. Sato, Y. Gao, et al., Unprecedented double C–C bond cleavage of a cyclopentadienyl ligand, *J. Am. Chem. Soc.* 125 (2003) 9568–9569.
- [43] C.H. Suresh, N. Koga, Aromaticity-driven rupture of CN triple and CC double bonds: Mechanism of the reaction between $Cp_2Ti(C_4H_4)$ and RCN, *Organometallics* 25 (2006) 1924–1931.
- [44] T.R. Hoye, B. Baire, D. Niu, et al., The hexadecyhydro-Diels–Alder reaction, *Nature* 490 (2012) 208–212.
- [45] D. Niu, P.H. Willoughby, B.P. Woods, et al., Alkane desaturation by concerted double hydrogen atom transfer to benzyne, *Nature* 501 (2013) 531–534.
- [46] I. Fernández, F.P. Cossío, Interplay between aromaticity and strain in double group transfer reactions to 1,2-benzyne, *J. Comput. Chem.* 37 (2016) 1265–1273.
- [47] D. Chen, D. Zhuang, Y. Zhao, et al., Reaction mechanisms of iron(III) catalyzed carbonyl–olefin metatheses in 2,5- and 3,5-hexadienals: significant substituent and aromaticity effects, *Org. Chem. Front.* 6 (2019) 3917–3924.
- [48] D. Zhuang, A.M. Rouf, Y. Li, et al., Aromaticity-promoted CO₂ capture by P/N-based frustrated Lewis pairs: a theoretical study, *Chem. Asian J.* 15 (2020) 266–272.
- [49] Y. Li, D. Zhuang, R. Qiu, et al., Aromaticity-promoted CS₂ activation by heterocycle-bridged P/N-FLPs: a comparative DFT study with CO₂ capture, *Phys. Chem. Chem. Phys.* 24 (2022) 2521–2526.
- [50] W.W. Chen, A. Cunillera, D. Chen, et al., Iodane-guided ortho C–H allylation, *Angew. Chem. Int. Ed.* 59 (2020) 20201–20207.
- [51] O. Eisenstein, J. Milani, R.N. Perutz, Selectivity of C–H activation and competition between C–H and C–F bond activation at fluorocarbons, *Chem. Rev.* 117 (2017) 8710–8753.
- [52] T. Shen, Q. Xie, Y. Li, et al., Aromaticity-promoted C–F bond activation in rhodium complex: a facile tautomerization, *Chem. Asian J.* 14 (2019) 1937–1940.
- [53] Q. Xie, Y. Zhao, D. Chen, et al., Probing reaction mechanism of [1,5]-migration in pyrrolidone and pyrrole derivatives: activation of a stronger bond in electropositive groups becomes easier, *Chem. Asian J.* 14 (2019) 2604–2610.
- [54] I.V. Alabugin, M. Manoharan, B. Breiner, et al., Control of kinetics and thermodynamics of [1,5]-shifts by aromaticity: A view through the prism of Marcus theory, *J. Am. Chem. Soc.* 125 (2003) 9329–9342.
- [55] J. Clarke, P.W. Fowler, S. Gronert, et al., Effect of ring size and migratory groups on [1,*n*] suprafacial shift reactions. Confirmation of aromatic and antiaromatic transition-state character by ring-current analysis, *J. Org. Chem.* 81 (2016) 8777–8788.
- [56] Q. Zhu, L. Lin, A.M. Rouf, et al., Reaction mechanisms on unusual 1,2-migrations of N-heterocyclic carbene-ligated transition metal complexes, *Chem. Asian J.* 14 (2019) 3313–3319.
- [57] Y. Li, J. Zhu, Achieving a favorable activation of the C–F bond over the C–H bond in five- and six-membered ring complexes by a coordination and aromaticity dually driven strategy, *Organometallics* 40 (2021) 3397–3407.
- [58] C. Castro, W.L. Karney, M.A. Valencia, et al., Möbius aromaticity in [12]annulene: Cis–Trans isomerization via twist-coupled bond shifting, *J. Am. Chem. Soc.* 127 (2005) 9704–9705.
- [59] H. Jiao, P.V.R. Schleyer, A detailed theoretical analysis of the 1,7-sigmatropic hydrogen shift: the Möbius character of the eight-electron transition structure, *Angew. Chem. Int. Ed.* 32 (1993) 1763–1765.
- [60] H.S. Rzepa, Double-twist Möbius aromaticity in a 4n + 2 electron electrocyclic reaction, *Chem. Commun.* (2005) 5220–5222.
- [61] M. Mauksch, S.B. Tsogoeva, A preferred disrotatory 4n electron Möbius aromatic transition state for a thermal electrocyclic reaction, *Angew. Chem. Int. Ed.* 48 (2009) 2959–2963.
- [62] A.Q. Cusumano, W.A. Goddard III, B.M. Stoltz, The transition metal catalyzed $\pi 2s + \pi 2s + \sigma 2s + \sigma 2s$ pericyclic reaction: Woodward–Hoffmann rules, aromaticity, and electron flow, *J. Am. Chem. Soc.* 142 (2020) 19033–19039.
- [63] J.-W. Zou, C.-H. Yu, Dyotropic rearrangements of dihalogenated hydrocarbons: a density functional theory study, *J. Phys. Chem. A* 108 (2004) 5649–5654.
- [64] I. Fernández, M.A. Sierra, F.P. Cossío, In-plane aromaticity in double group transfer reactions, *J. Org. Chem.* 72 (2007) 1488–1491.
- [65] A.G. Algarra, Computational insights into the S₃ transfer reaction: a special case of double group transfer reaction featuring bicyclically delocalized aromatic transition state geometries, *J. Comput. Chem.* 38 (2017) 1966–1973.
- [66] D. Zhuang, Y. Li, J. Zhu, Antiaromaticity-promoted activation of dihydrogen with borole fused cyclooctatetraene frustrated Lewis pairs: a density functional theory study, *Organometallics* 39 (2020) 2636–2641.
- [67] J.J. Cabrera-Trujillo, I. Fernández, Aromaticity can enhance the reactivity of P-donor/borole frustrated Lewis pairs, *Chem. Commun.* 55 (2019) 675–678.
- [68] J.J. Cabrera-Trujillo, I. Fernández, Aromaticity-enhanced reactivity of geminal frustrated Lewis pairs, *Chem. Commun.* 58 (2020) 6801.
- [69] B.J. Levandowski, N.S. Abularrage, K.N. Houk, et al., Hyperconjugative antiaromaticity activates 4H-pyrazoles as inverse-electron-demand Diels–Alder dienes, *Org. Lett.* 21 (2019) 8492–8495.
- [70] S.R.D. George, T.E. Eltona, J.B. Harper, Electronic effects on the substitution reactions of benzhydrols and fluorenyl alcohols. Determination of mechanism and effects of antiaromaticity, *Org. Biomol. Chem.* 13 (2015) 10745–10750.
- [71] B.J. Levandowski, K.N. Houk, Hyperconjugative, secondary orbital, electrostatic, and steric effects on the reactivities and endo and exo stereoselectivities of cyclopropane Diels–Alder reactions, *J. Am. Chem. Soc.* 138 (2016) 16731–16736.
- [72] B.J. Levandowski, L. Zou, K.N. Houk, Hyperconjugative aromaticity and antiaromaticity control the reactivities and π -facial stereoselectivities of 5-substituted cyclopentadiene Diels–Alder cycloadditions, *J. Org. Chem.* 83 (2018) 14658–14666.
- [73] S. Winstein, M. Shatavsky, C. Norton, et al., 7-Norbornenyl and 7-norbornyl cations, *J. Am. Chem. Soc.* 77 (1955) 4183–4184.
- [74] T. Slanina, R. Ayub, J. Toldo, et al., Impact of excited-state antiaromaticity relief in a fundamental benzene photoreaction leading to substituted bicyclo[3.1.0]hexenes, *J. Am. Chem. Soc.* 142 (2020) 10942–10954.
- [75] M. Ueda, K. Jorner, Y.M. Sung, et al., Energetics of Baird aromaticity supported by inversion of photoexcited chiral [4*n*]annulene derivatives, *Nat. Commun.* 8 (2017) 346.
- [76] A.K. Narsaria, T.A. Hamlin, K. Lammertsma, et al., Dual activation of aromatic Diels–Alder reactions, *Chem. Eur. J.* 25 (2019) 9902–9912.

- [77] M. Culka, S.G. Huwiler, M. Boll, et al., Breaking benzene aromaticity—computational insights into the mechanism of the tungsten-containing benzoyl-CoA reductase, *J. Am. Chem. Soc.* 139 (2017) 14488–14500.
- [78] M. Garcia-Borràs, S. Osuna, M. Swart, et al., Electrochemical control of the regioselectivity in the exohedral functionalization of C_{60} : the role of aromaticity, *Chem. Commun.* 49 (2013) 1220–1222.
- [79] O.E. Bakouri, M. Garcia-Borràs, R.M. Girón, et al., On the regioselectivity of the Diels–Alder cycloaddition to C_{60} in high spin states, *Phys. Chem. Chem. Phys.* 20 (2018) 11577–11585.
- [80] M. Garcia-Borràs, M.R. Cerón, S. Osuna, et al., The regioselectivity of Bingel–Hirsch cycloadditions on isolated pentagon rule endohedral metallofullerenes, *Angew. Chem. Int. Ed.* 55 (2016) 2374–2377.
- [81] Y. Ni, Y. Lu, K. Zhang, et al., Aromaticity/antiaromaticity effect on activity of transition metal macrocyclic complexes towards electrocatalytic oxygen reduction, *ChemSusChem* 14 (2021) 1835–1839.
- [82] K. Xiao, Y. Zhao, J. Zhu, et al., Hyperconjugative aromaticity and protodeauration reactivity of polyaureated indoliums, *Nat. Commun.* 10 (2019) 5639.
- [83] Z. Wang, Y. Zhou, J.-X. Zhang, et al., DFT studies on the reactions of boroles with alkynes, *Chem. Eur. J.* 24 (2018) 9612–9621.
- [84] Z. Lu, H. Hausmann, S. Becker, et al., Aromaticity as stabilizing element in the bidentate activation for the catalytic reduction of carbon dioxide, *J. Am. Chem. Soc.* 137 (2015) 5332–5335.
- [85] A.M. Rouf, C. Dai, F. Xu, et al., Dinitrogen activation by tricoordinated boron species: a systematic design, *Adv. Theory Simul.* 3 (2020) 1900205.
- [86] A.M. Rouf, Y. Huang, S. Dong, et al., Systematic design of a frustrated Lewis pair containing methyleneborane and carbene for dinitrogen activation, *Inorg. Chem.* 60 (2021) 5598–5606.
- [87] J.R. Bleeke, *Metallabenzenes*, *Chem. Rev.* 101 (2001) 1205–1228.
- [88] I. Fernández, G. Frenking, G. Merino, Aromaticity of metallabenzenes and related compounds, *Chem. Soc. Rev.* 44 (2015) 6452–6463.
- [89] D. Chen, Y. Hua, H. Xia, *Metallaaromatic chemistry: history and development*, *Chem. Rev.* 120 (2020) 12994–13086.
- [90] Y. Zhang, C. Yu, Z. Huang, et al., Metalla-aromatics: planar, nonplanar, and Spiro, *Acc. Chem. Res.* 54 (2021) 2323–2333.
- [91] J. Chen, G. Jia, Recent development in the chemistry of transition metal-containing metallabenzene and metallabenzynes, *Coord. Chem. Rev.* 257 (2013) 2491–2521.
- [92] C. Zhu, S. Li, M. Luo, et al., Stabilization of anti-aromatic and strained five-membered rings with a transition metal, *Nat. Chem.* 5 (2013) 698–703.
- [93] C. Zhu, X. Zhou, H. Xing, et al., σ -Aromaticity in an unsaturated ring: osmapentadiene derivatives containing a metallacyclopropene unit, *Angew. Chem. Int. Ed.* 54 (2015) 3102–3106.
- [94] C. Zhu, Q. Zhu, J. Fan, et al., A metal-bridged tricyclic aromatic system: synthesis of osmium polycyclic aromatic complexes, *Angew. Chem. Int. Ed.* 53 (2014) 6232–6236.
- [95] Y. Cai, Y. Hua, Z. Lu, et al., Electrophilic aromatic substitution reactions of compounds with Craig–Möbius aromaticity, *Proc. Natl. Acad. Sci. U.S.A.* 118 (2021) e2102310118.
- [96] J. Lin, L. Ding, Q. Zhuo, et al., Formal [2+2+2] cycloaddition reaction of a metal-carbyne complex with nitriles: synthesis of a metallapyrazine complex, *Organometallics* 25 (2019) 5077–5085.
- [97] A. Roglans, A. Pla-Quintana, M. Solà, Mechanistic studies of transition-metal-catalyzed [2 + 2 + 2] cycloaddition reactions, *Chem. Rev.* 121 (2021) 1894–1979.
- [98] Z. Lu, Q. Zhu, Y. Cai, et al., Access to tetracyclic aromatics with bridgehead metals via metalla-click reactions, *Sci. Adv.* 6 (2020) eaay2535.
- [99] Z. Chu, G. He, X. Cheng, et al., Synthesis and characterization of cyclopropa-*o*-manaphthalenes containing a fused σ -aromatic metallacyclopropene unit, *Angew. Chem. Int. Ed.* 58 (2019) 9174–9178.
- [100] Q. Zhuo, J. Lin, Y. Hua, et al., Multiyne chains chelating osmium via three metal-carbon σ bonds, *Nat. Commun.* 8 (2017) 1912.
- [101] Z. Lu, C. Zhu, Y. Cai, et al., Metallapentalenofurans and lactone-fused metallapentalynes, *Chem. Eur. J.* 23 (2017) 6426–6431.
- [102] K. Zhuo, Y. Liu, K. Ruan, et al., Ring contraction of metallacyclobutadiene to metallacyclopropene driven by π - and σ -aromaticity relay, *Nat. Synth.* 2 (2023) 67–75.
- [103] C. Foroutan-Nejad, Is NICS a reliable aromaticity index for transition metal clusters? *Theor. Chem. Acc.* 134 (2015) 8.
- [104] A. Benallou, H.E.A.E. Abdallaoui, The aromatic character of the transition state structures (TSs) involved in pseudocyclic reactions of fluorinated compounds, *J. Fluor. Chem.* 229 (2020) 109421.
- [105] R. Papadakis, H. Ottosson, The excited state antiaromatic benzene ring: a molecular Mr Hyde? *Chem. Soc. Rev.* 44 (2015) 6472–6493.
- [106] S. Gupta, S. Su, Y. Zhang, et al., Ruthenabenzene: a robust precatalyst, *J. Am. Chem. Soc.* 143 (2021) 7490–7500.
- [107] F.H. Cui, Y. Hua, Y.-M. Lin, et al., Selective difunctionalization of unactivated aliphatic alkenes enabled by a metal–metallaaromatic catalytic system, *J. Am. Chem. Soc.* 144 (2022) 2301–2310.



Qian Zhu received her B.S. degree from Zhengzhou University in 2012 and earned her M.S. degree (Supervisor: Prof. Haiping Xia) and Ph.D. degree (Supervisor: Prof. Jun Zhu) from Xiamen University in 2015 and 2020, respectively. From 2020 to 2022, she worked as a postdoctor at Nanjing University (Supervisor: Prof. Jing Ma). Currently, she works at Nanjing University of Posts and Telecommunications. Her research interests focus on the inert bond activation and machine learning models for data-driven material designs.



Jun Zhu (BRID: 09855.00.09697) is currently a professor of School of Science and Engineering at the Chinese University of Hong Kong, Shenzhen. He obtained the B.S and Ph.D. degrees from Xiamen University and the Hong Kong University of Science and Technology in 2000 and 2007, respectively. Then he moved to Hong Kong University and Uppsala University for the postdoctoral study. In 2010, he joined the Department of Chemistry at Xiamen University and was promoted to a full professor in 2018. In 2023, he moved to the Chinese University of Hong Kong, Shenzhen. His research group (<http://junzhu.chem8.org>) focuses mainly on aromaticity and small molecule activation including dinitrogen. His motto is “Enjoy chemistry & life to explore the unknown world”.